

Exclusive vector-quarkonium photoproduction at NLO in α_s in collinear factorisation with evolution of the generalised parton distributions and high-energy resummation

C.A. Flett ^a, J.P. Lansberg ^a, S. Nabeebaccus ^a, M. Nefedov ^a, P. Sznajder ^b, J. Wagner ^b

^aUniversité Paris-Saclay, CNRS, IJCLab, 91405 Orsay, France

^bNational Centre for Nuclear Research (NCBJ), Pasteura 7, 02-093 Warsaw, Poland

Abstract

We perform the first complete one-loop study of exclusive photoproduction of vector quarkonia off protons in Collinear Factorisation (CF) including the scale evolution of the Generalised Parton Distributions (GPDs). We confirm the perturbative instability of the cross section at high photon-proton-collision energies ($W_{\gamma p}$) at Next-to-Leading Order (NLO) in α_s and solve this issue by resumming higher-order QCD corrections, which are enhanced by a logarithm of the parton energies, using High-Energy Factorisation (HEF) in the Doubly-Logarithmic Approximation (DLA) matched to CF. Our NLO CF \oplus DLA HEF results are in agreement with the latest HERA data, show a smaller sensitivity to the factorisation and renormalisation scales compared to Born-order results. Quark-induced channels via interference with gluon ones are found to contribute at most 20% of the cross section for $W_{\gamma p} > 100$ GeV. Our results also show that such exclusive cross sections cannot be accurately obtained from the square of usual Parton Distribution Functions (PDFs) and clearly illustrate the importance of quarkonium exclusive photoproduction to advance our understanding of the 3D content of the nucleon in terms of gluons. Our work provides an important step towards a correct interpretation of present and future experimental data collected at HERA, the EIC, the LHC and future experiments.


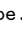
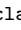



Keywords: J/ψ , Υ , exclusive photoproduction, HERA, EIC, LHC, LHeC, FCC-eh, EIC, NLO, high-energy resummation

1. Introduction

Hard exclusive reactions are complementary to inclusive reactions such as Deep-Inelastic Scattering (DIS) in order to probe the inner content of the hadrons and study the strong interaction. A class of such hard exclusive reactions is of particular interest as they probe the 3D hadron structure through Generalised Parton Distributions (GPDs) [1–3] which extend the usual 1D Parton Distribution Functions (PDFs) of Collinear Factorisation (CF) used for single-scale hard-inclusive reactions like DIS.

One such process is exclusive Deeply-Virtual-Meson-Production (DVMP) off protons, initiated by a longitudinally polarised photon, $\gamma_L^*(q)p_s(p) \rightarrow M(p_M)p'_{s'}(p')$, see Fig. 1. This process admits, at small $t = (p' - p)^2$ and in the massless-quark limit, a collinear factorisation [4] at the level of the amplitude, $\mathcal{A}_{ss'}$, as a double convolution of (i) a process-dependent perturbative hard-scattering coefficient function, C_i , (ii) a universal, non-perturbative meson distribution amplitude (DA), ϕ , and (iii) a universal, non-perturbative quark and/or gluon GPD correlator $F_{i,ss'}$ ($i = q, g$), as

$$\mathcal{A}_{ss'} = F_{i,ss'}(x, \xi, t; \mu_F) \otimes C_i(x, \xi, z; \mu_F, \mu_R) \otimes \phi_M(z; \mu_F). \quad (1)$$

Email addresses: Christopher.Flett@ijclab.in2p3.fr (C.A. Flett ) , Jean-Philippe.Lansberg@ijclab.in2p3.fr (J.P. Lansberg ) , Saad.Nabeebaccus@ijclab.in2p3.fr (S. Nabeebaccus ) , Maxim.Nefedov@ijclab.in2p3.fr (M. Nefedov ) , Pawel.Sznajder@ncbj.gov.pl (P. Sznajder ) , Jakub.Wagner@ncbj.gov.pl (J. Wagner )

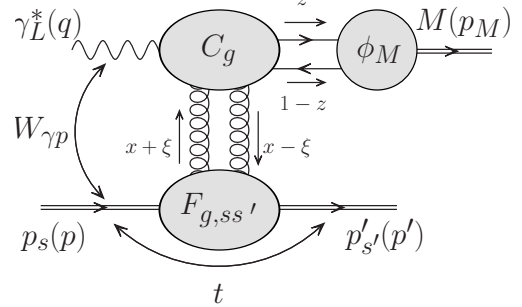


Figure 1: Factorisation of the amplitude for DVMP in the gluon channel.

Here, \otimes denotes the sum of the flavour, spin and colour of the exchanged partons, and the convolution over x and z , with z being the fraction of the meson M momentum carried by the quark, and x being the average momentum fraction of the nucleon p carried by the parton i . In addition, $\Delta = (p' - p)$ is the momentum transfer and¹ $\xi = \Delta^+ / 2P^+$ ($P = (p + p')/2$) is the fraction of the longitudinal proton momentum transfer, or skewness. The presence of x , ξ and t in F underlies the factorisation in terms of 3D GPDs rather than the usual 1D PDFs and the presence of μ_F is due to the fact that both GPDs and DAs are subject to evolution equations.

¹Here, the light-cone components are defined as $k^\pm \equiv (k^0 \pm k^3) / \sqrt{2}$ and $\mathbf{k}_\perp \equiv (k^1, k^2)$ in the γp center-of-momentum frame, with the z axis defined along the proton direction.

In the light-cone gauge and at leading twist, F_q and F_g are Fourier transforms of matrix elements of chiral-even operators constructed from quark fields ψ^q or gluon-field-strength tensors $F^{\mu\nu}$ as follows (with $y^+ = 0$ and $\mathbf{y}_\perp = \mathbf{0}$):

$$\begin{aligned} F_{q,ss'} &= \frac{1}{2} \int \frac{dy^-}{2\pi} e^{ixP^+y^-} \langle p', s' | \bar{\psi}^q \left(\frac{-y}{2} \right) \gamma^+ \psi^q \left(\frac{y}{2} \right) | p, s \rangle, \\ F_{g,ss'} &= \frac{1}{P^+} \int \frac{dy^-}{2\pi} e^{ixP^+y^-} \langle p', s' | F^{+\mu} \left(\frac{-y}{2} \right) F_\mu^+ \left(\frac{y}{2} \right) | p, s \rangle. \end{aligned} \quad (2)$$

In practice, they are parametrised via specific Lorentz structures and twist-2 parton-helicity conserving GPDs $H^{q,g}(x, \xi, t; \mu_F)$ and $E^{q,g}(x, \xi, t; \mu_F)$, as follows ($j = q, g$)

$$F_{j,ss'} = \frac{1}{2P^+} \left[\bar{u}_{s'}(p') \left(H_j \gamma^+ + E_j \frac{i\sigma^{+\Delta}}{2m_p} \right) u_s(p) \right]. \quad (3)$$

Although not formally proven to all orders in perturbative QCD (pQCD), the same factorisation theorem is assumed for photoproduction (i.e. quasi-real photons with virtuality $q^2 \approx 0$) of heavy vector quarkonia, $\gamma p \rightarrow \mathcal{Q} p$, where $\mathcal{Q} = J/\psi, \Upsilon, \dots$, due to the hard scale provided by the heavy-quark mass m_Q . Explicit one-loop computations in the non-relativistic static limit, where the DA $\phi_M(z; \mu_F)$ reduces to $\delta(z - 1/2)$, have shown that factorisation holds up to NLO in α_s [5]. This also applies for off-shell photons [6]. While the LO cross section uniquely depends on gluon GPDs, sensitivity to quark GPDs arises at NLO along with explicit renormalisation (μ_R) and factorisation (μ_F) scale dependences.

However, the corresponding NLO cross sections are very sensitive to μ_F for $W_{\gamma p} \gg m_Q$, like for several inclusive quarkonium observables [7–9]. In these inclusive reactions, this has been resolved either by fixing μ_F to reduce anomalously large NLO corrections [10, 11] or by resumming the high-energy logarithms responsible for these perturbative instabilities using High-Energy Factorisation (HEF) [12, 13]. Here, we aim to demonstrate that a similar resummation also cures the issue in exclusive reactions, going beyond the scale-fixing criterion advocated in [14] and to perform a complete phenomenological study with GPD evolution, including comparisons to precise HERA data.

The structure of this Letter is as follows: Section 2 reviews CF formulae at fixed order in α_s , identifies the origin of the perturbative instabilities at NLO, and explains our GPD modelling and evolution set up. Section 3 explains HEF resummation and the limitations of a scale-fixing criterion beyond NLO. Section 4 compares our results to experimental data and analyses resummation effects on scale dependencies. Section 5 discusses connections with other approaches using forward limits. Section 6 gathers our conclusions.

2. Exclusive photoproduction of vector quarkonia in collinear factorisation

2.1. GPD modelling and evolution

A very convenient procedure to construct models of GPDs encapsulating all their properties is to use double distributions [1], $f_i(\beta, \alpha)$, where $i = q, g$. These distributions

are related to GPDs in the following way:

$$H_i(x, \xi; \mu_0) = \int_{-1}^1 d\beta \int_{-1+|\beta|}^{1-|\beta|} d\alpha \delta(\beta + \xi\alpha - x) f_i(\beta, \alpha; \mu_0). \quad (4)$$

Assuming that $f_i(\beta, \alpha)$ are even functions of α , polynomiality of GPDs, which is a consequence of Lorentz invariance (see e.g. Ref. [15]), is automatically satisfied.

One can further ensure the proper forward limits² of the GPDs, connecting them to PDFs, by the following common factorisation Ansatz [16, 17]:

$$f_i(\beta, \alpha; \mu_0) = h_i(\beta, \alpha) \times \begin{cases} |\beta| g(|\beta|; \mu_0) & \text{for } i = g, \\ \theta(\beta) q_{\text{val}}(|\beta|; \mu_0) & \text{for valence } q, \\ \text{sgn}(\beta) q_{\text{sea}}(|\beta|; \mu_0) & \text{for sea } q, \end{cases} \quad (5)$$

where $g(x)$ is the gluon PDF, $q_{\text{val}}(x)$ and $q_{\text{sea}}(x)$ are the valence and sea components of quark PDFs and $h_i(\beta, \alpha)$ is the so-called profile function satisfying

$$\int_{-1+|\beta|}^{1-|\beta|} d\alpha h_i(\beta, \alpha) = 1, \quad (6)$$

as originally proposed in [18, 19]. A popular choice for $h_i(\beta, \alpha)$ is then [20]:

$$h_i(\beta, \alpha) \equiv \frac{\Gamma(2n_i + 2)}{2^{2n_i+1} \Gamma^2(n_i + 1)} \frac{\left((1 - |\beta|)^2 - \alpha^2 \right)^{n_i}}{(1 - |\beta|)^{2n_i+1}}, \quad (7)$$

where the parameter n_i (which can be flavour-dependent) controls the width of the profile function and, effectively, the buildup of the skewness effect. In particular, for $n \rightarrow \infty$, the ξ dependence of such a GPD disappears, i.e. $h_q(\beta, \alpha)|_{n \rightarrow \infty} = \delta(\alpha)$ and therefore $H_q(x, \xi; \mu_0)|_{n \rightarrow \infty} = q(x; \mu_0)$.

Along the same lines, a t dependence can easily be implemented, while keeping the same limiting behaviours, by extending $h_i(\beta, \alpha)$ to $h_i(\beta, \alpha, t)$ satisfying $\lim_{t \rightarrow 0} h_i(\beta, \alpha, t) = h_i(\beta, \alpha)$. In the Goloskokov-Kroll (GK) DD model [21], which we use here, it is done via a simple exponential dependence in t such that $h_i(\beta, \alpha, t) \equiv e^{bt} h_i(\beta, \alpha)$ while $n_g = n_q^{\text{sea}} = 2$ and $n_q^{\text{val}} = 1$. Instead of using the CTEQ6M PDF set [22] as the forward inputs as in [21], one can use more modern PDF sets. For most of our results, we will use the central set of CT18NLO [23]. As we explain in the next section, we focus on the differential cross section at the minimum value of $|t|$, $t_{\min} = -4\xi^2 m_p^2 / (1 - \xi^2)$ which, at large $W_{\gamma p}$ where $\xi \simeq M_Q^2 / (2W_{\gamma p}^2)$, becomes $t_{\min} \simeq -m_p^2 M_Q^4 / W_{\gamma p}^4$ and is thus extremely small compared to the other hadronic scales. As such, we do not need to model the t dependence of GPDs.

This DD model has been implemented in the PARTONS framework [24] interfaced to the APFEL++ code [25] for performing the full leading-logarithmic (LL) GPD evolution with kernels at one-loop [26] and has been used at $\mu_0 = 2$ GeV as our initial condition for the GPD evolution.

² $H_g(\pm x, 0; \mu_F) = xg(x; \mu_F)$ and $H_q(x, 0; \mu_F) = q(x; \mu_F)$, $H_q(-x, 0; \mu_F) = -\bar{q}(x; \mu_F)$ for $x > 0$.

We note that modelling GPDs with DDs only allows one to study a class of GPD models. In particular, they do not allow one to include contributions with the largest ξ power which are usually modelled by the so-called D term [27]. At large $W_{\gamma p}$ (thus small ξ) which is our focus here, these are, however, not expected to be relevant.

2.2. Coefficient functions and cross sections in Collinear Factorisation

Following Ref. [6], we write the quarkonium photoproduction amplitude in CF at leading twist in the form:

$$\mathcal{A}_{ss'}^{\lambda\lambda'} = -\varepsilon_\lambda^\gamma \varepsilon_{\lambda'}^{*Q} \sum_{i=q,s} \int_{-1}^1 \frac{dx}{x^{1+\delta_{ig}}} C_i(x, \xi; \mu_F, \mu_R) F_{i,ss'}(x, \xi, t; \mu_F), \quad (8)$$

where $\varepsilon_\lambda^\gamma$ is the photon-polarisation vector with helicity λ in the gauge $\varepsilon_\lambda^\gamma \cdot p = 0$ and $\varepsilon_{\lambda'}^Q$ that of the quarkonium. In Eq. (8), the integration over $x \in [-1, 1]$ covers the so-called DGLAP region (with $\xi < |x| < 1$) and the ERBL region (with $|x| < \xi < 1$), two distinct regions where the GPDs obey two different evolution equations [26].

We first note that the t dependence of the CF amplitude only explicitly appears through the GPD F_i . Since the gluon GPDs giving the largest contribution to quarkonium photoproduction are poorly known and their t dependence essentially unknown, we will limit ourselves to $t = t_{\min}$ which can in practice be approximated to zero for the $W_{\gamma p}$ values attainable at the EIC, HERA and the LHC in Ultra-Peripheral Collisions (UPCs). Precise HERA data [28] for $t \simeq 0$ as a function of $W_{\gamma p}$ are available and are sufficient for the data-theory comparison we aim at. We leave discussions on the t dependence and of the t -integrated cross sections for a future work³.

As we announced, at LO in α_s and in the squared relative velocity of the heavy quarks, v^2 , the gluon coefficient function (unlike the quark one) is nonzero:

$$C_g^{(0)}(x, \xi; \mu_R) = \frac{x^2 c}{(x + \xi - i\varepsilon)(x - \xi + i\varepsilon)}, \quad (9)$$

where $c = (4\pi\alpha_s(\mu_R)ee_Q R_Q(0))/(m_Q^{3/2} \sqrt{2\pi N_c})$. In the above, $R_Q(0)$ is the value at the origin of the spatial radial wave function⁴ of the quarkonium Q , e_Q is the electric charge of the heavy quark Q in units of the positron charge and e is the positron charge in natural units. The heavy-quark mass m_Q is chosen to be $M_Q/2$ and we choose $R_{J/\psi}(0) = 1 \text{ GeV}^{3/2}$ and $R_\Upsilon(0) = 3 \text{ GeV}^{3/2}$ in the range of potential-model values [29, 30]. A two-loop CRunDec [31] running of α_s with $\alpha_s(M_Z^2) = 0.118$ is employed.

³The $\gamma p \rightarrow Qp$ two-body t -differential cross section is readily obtained from the amplitude Eq. (8) as usual from $d\sigma/dt = 1/(16\pi(W_{\gamma p}^2 - m_p^2)^2) \sum_{\lambda, \lambda' = \pm} \sum_{s, s'} |\mathcal{A}_{ss'}^{\lambda\lambda'}|^2$, where the sums include the initial-state averaging over the incoming proton spins (s, s') and the photon transverse helicities (\pm). σ is then obtained by integrating from t_{\min} to $-\infty$.

⁴It is the solution of the non-relativistic Schrödinger equation.

At small ξ (or large $W_{\gamma p}$) and finite x , the NLO coefficient functions $C_{g,q}^{(1)}(x, \xi; \mu_R, \mu_F)$ first obtained in [5] scale like

$$-\frac{i\pi c|x|}{2\xi} \frac{\alpha_s(\mu_R)}{\pi} \ln\left(\frac{m_Q^2}{\mu_F^2}\right) \left\{ C_A, 2C_F \right\} \equiv C_{\{g,q\}}^{(1, \text{asy.})}(x, \xi; \mu_R, \mu_F). \quad (10)$$

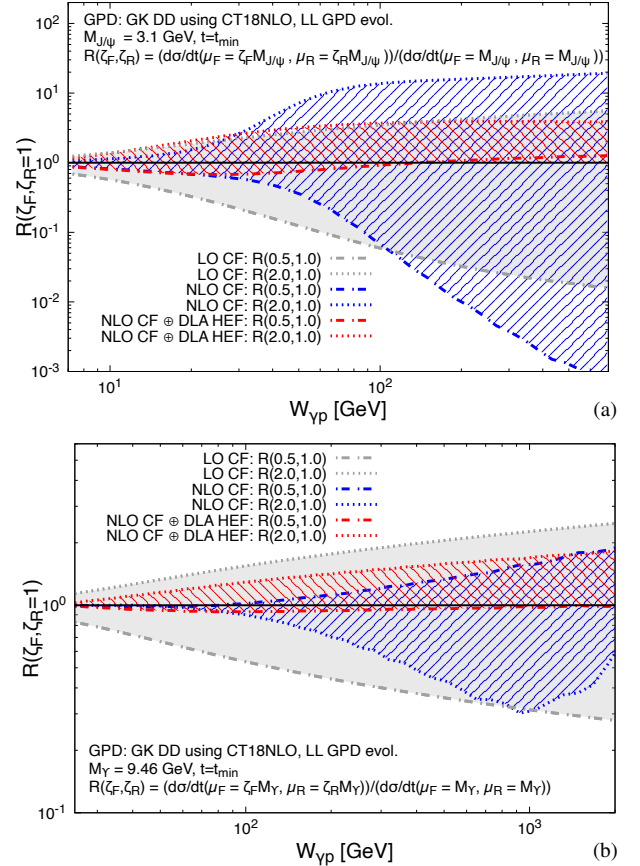


Figure 2: μ_F scale uncertainty of the LO CF, NLO CF and NLO CF \oplus DLA HEF (a) J/ψ and (b) Υ t -differential cross sections at t_{\min} .

Since the x dependence of the gluon GPD F_g is close to a constant for $\mu_F \sim 2 - 3 \text{ GeV}$ relevant for J/ψ , the corresponding NLO contribution⁵ to the amplitude (8) is enhanced by $\ln(1/\xi)$ at small ξ , as observed already in Ref. [5]. This leads to the catastrophically large μ_F dependence shown in Fig. 2a of the NLO CF (blue) J/ψ cross section compared to the LO (grey) one at large $W_{\gamma p}$. The same observation can hardly be made for the Υ case (Fig. 2b) which sits at a larger scale leading to F_g decreasing with ξ and to a smaller α_s . Note that the LO CF uncertainty increases with $W_{\gamma p}$ due to GPD evolution (in particular the singular behaviour of P_{gg}).

For $\mu_F = m_Q$, $C_{g,q}^{(1, \text{asy.})} = 0$. Such a scale choice (denoted $\hat{\mu}_F$ here) corresponds [14] to the resummation of a series of corrections to the amplitude $\propto (\alpha_s \ln(\mu_F/m_Q) \ln(1/\xi))^n$, used in phenomenological analyses [32–34], but misses all

⁵A similar reasoning holds for the (NLO) quark contributions with the flavour-singlet GPD scaling like $1/x$.

corrections $\propto (\alpha_s \ln(1/\xi))^n$ without $\ln(\mu_F)$. A similar scale-fixing prescription was advocated for P_T -integrated cross sections of *inclusive* hadro- [10] and photoproduction [11] of heavy quarkonia. As noted in [10], certain conventional gluon PDFs exhibit a local minimum in x close to 10^{-3} for μ_F values below 2 GeV. In DD models⁶, this behaviour leads to oscillating GPDs in x , via the forward-limit constraints, and results in an unusual energy-dependence of the exclusive J/ψ photoproduction cross section. We however leave this issue to future investigation as it does not relate to the hard-scattering properties but rather to the GPD modelling.

3. Resummation via High-Energy Factorisation

3.1. The resummed CF coefficient functions

At higher orders in α_s , the CF coefficient function, $C_i(x, \xi; \mu_F, \mu_R)$, written in terms of the variable $\rho = \xi/x$, develops [5, 38] a series of corrections $\propto (\alpha_s^n \ln^{n-1}(1/|\rho|))/|\rho|$ which become important at $|\rho| \ll 1$ and whose consideration leads to the Leading-Logarithmic Approximation (LLA). This series can be resummed using the *High-Energy Factorisation* formalism of Refs. [39–42], originally developed for *inclusive* processes. The application of this formalism to *exclusive* processes is possible due to the optical theorem, as explained in the next paragraph.

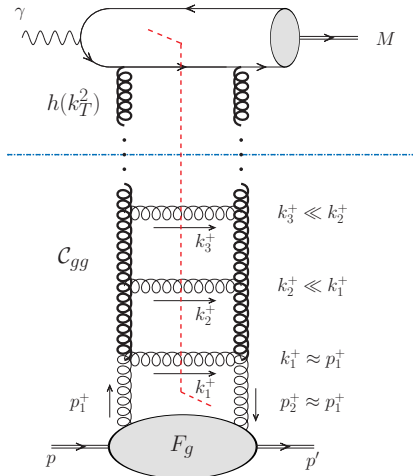


Figure 3: Typical Feynman diagram contributing to the imaginary part of the photoproduction amplitude (8) in the $\rho \ll 1$ region in the LLA. The thick gluons in the t channel are Reggeised. Further notation is explained in the text.

The typical Feynman diagram and loop-momentum region contributing to the imaginary part in the LLA is shown in Fig. 3, where the gluons depicted by thick helices, connecting emissions strongly ordered in k^+ , are the so-called *Reggeised gluons*; these are the effective gauge-invariant degrees of freedom of high-energy QCD whose operator definition can be given e.g. by the Lipatov high-energy

EFT [43] or the approach of Ref. [44], which is equivalent up to NLLA. One notes that the part of the cut diagram below the horizontal dash-dotted line in Fig. 3 is just the usual inclusive BFKL ladder [45–47] which is integrated over the transverse momenta of all emitted gluons, including the most energetic emission k_1 . Collinear divergences from the $\mathbf{k}_{i\perp}$ integrations (Fig. 3) should be subtracted according to the $\overline{\text{MS}}$ scheme to comply with the collinear GPD definition. This challenging computation [39, 40, 42] corresponds to the part of the diagram in Fig. 3 below the horizontal dash-dotted line, i.e. the HEF resummation factor $C_{gi}(\rho, \mathbf{k}_\perp^2; \mu_F, \mu_R)$. This factor has been proven to be process-independent within the LLA [48] and the NLLA [49] in $\ln(1/|\rho|)$. In the quark channel, one has within the LLA,

$$C_{gq} = \frac{2C_F}{C_A} [C_{gg} - \delta(\rho - 1)\delta(\mathbf{k}_\perp^2)], \quad (11)$$

where the overall factor of 2 is confirmed by a detailed computation in Appendix A.

Indeed, the process-dependent HEF coefficient function $h(\mathbf{k}_\perp^2)$, depicted diagrammatically above the dash-dotted line in Fig. 3, does not contain any large logarithms of $\ln(1/|\rho|)$. As a result, at leading power in $|\rho| \ll 1$, the resummed coefficient function, which is meant to replace C_i in Eq. (8), factorises as follows [38, 50]:

$$C_i^{(\text{HEF})}(\rho; \mu_F, \mu_R) = \frac{-i}{|\rho|} \int_0^\infty d\mathbf{k}_\perp^2 C_{gi}(|\rho|, \mathbf{k}_\perp^2; \mu_F, \mu_R) h(\mathbf{k}_\perp^2), \quad (12)$$

with the well known (see e.g. [38, 51]) HEF coefficient function at LO in α_s :

$$h(\mathbf{k}_\perp^2) = \frac{\pi c}{2} \frac{m_Q^2}{m_Q^2 + \mathbf{k}_\perp^2}. \quad (13)$$

For completeness, we provide the details of the derivation of this result in Appendix A, which to our knowledge are not present in the literature.

The function C_{gi} in the complete LLA includes [39–42] some μ_F -dependent terms which will not be compensated by the fixed-order evolution of GPDs, see Sec. 2.3 of Ref. [12]. Therefore, to stay consistent with GPD evolution, we truncate the LLA down to the *doubly-logarithmic approximation (DLA)* which resums only corrections proportional to $(\alpha_s(\mu_R) \ln(1/\rho) \ln(\mu_F^2/\mathbf{k}_\perp^2))^n$ in C_{gi} , and has the following Mellin representation in the gluon channel [41, 52]:

$$C_{gg}^{(\text{DL})}(\rho, \mathbf{k}_\perp^2) = \int \frac{dN}{2\pi i} \rho^{-N} \frac{\gamma_N}{\mathbf{k}_\perp^2 \left(\frac{\mathbf{k}_\perp^2}{\mu_F^2}\right)^{\gamma_N}}, \quad (14)$$

with $\gamma_N = \hat{\alpha}_s(\mu_R)/N$ with $\hat{\alpha}_s = \alpha_s C_A/\pi$. The Mellin transform in Eq. (14) maps the logarithms of $1/\rho$ to poles at $N = 0$: $\ln^{k-1} \frac{1}{\rho} \leftrightarrow \frac{(k-1)!}{N^k}$.

Substituting Eq. (14) into Eq. (12), one obtains the following Mellin-space result for the resummed coefficient function in the DLA HEF:

$$C_g^{(\text{DLA HEF})}(N) = \frac{-i\pi c}{2} \left(\frac{m_Q^2}{\mu_F^2}\right)^{\gamma_N} \frac{\pi\gamma_N}{\sin(\pi\gamma_N)}. \quad (15)$$

⁶The same would apply to the case of GPDs obtained with the Shuvaev transform [35–37].

which, expanded in α_s up to NNLO, reads in ρ space (with an overall factor $-i\pi c/2$):

$$\delta(|\rho| - 1) + \frac{\hat{\alpha}_s}{|\rho|} \ln\left(\frac{m_D^2}{\mu_F^2}\right) + \frac{\hat{\alpha}_s^2}{|\rho|} \ln\left[\frac{1}{|\rho|} \left[\frac{\pi^2}{6} + \frac{1}{2} \ln^2\left(\frac{m_D^2}{\mu_F^2}\right)\right]\right]. \quad (16)$$

The α_s^0 and α_s^1 terms respectively agree with the imaginary part of $C_g^{(0)}$ and $C_g^{(1, \text{asy.})}$. Using Eq. (11), one obtains a similar correspondence for $C_q^{(1, \text{asy.})}$. Up to NNLO in α_s , the DLA coincides with the complete LLA so the prediction of the NNLO term in the coefficient function in Eq. (16) is exact.

The inverse Mellin transform of Eq. (15), after subtraction⁷ of the α_s^0 term, can be cast into the following all-order expression in ρ space, for $L_\mu \equiv \ln[m_D^2/\mu_F^2] > 0$:⁸

$$\check{C}_g^{(\text{HEF})}(\rho) = \frac{-i\pi c \hat{\alpha}_s}{2 |\rho|} \sqrt{\frac{L_\mu}{L_\rho}} \times \quad (17)$$

$$\left\{ I_1\left(2\sqrt{L_\rho L_\mu}\right) - 2 \sum_{k=1}^{\infty} \text{Li}_{2k}(-1) \left(\frac{L_\rho}{L_\mu}\right)^k I_{2k-1}\left(2\sqrt{L_\rho L_\mu}\right) \right\},$$

where $L_\rho \equiv \hat{\alpha}_s \ln 1/|\rho|$. For $L_\mu < 0$, $\check{C}_g^{(\text{HEF})}(\rho)$ is obtained from the replacement $\sqrt{L_\mu/L_\rho} I_{2k-1}(2\sqrt{L_\rho L_\mu}) \rightarrow (-1)^k \sqrt{(-L_\mu)/L_\rho} J_{2k-1}(2\sqrt{-L_\mu L_\rho})$. In addition, one has $\check{C}_q^{(\text{HEF})}(\rho) = \frac{2C_F}{C_A} \check{C}_g^{(\text{HEF})}(\rho)$.

The low- ρ behaviour of $\check{C}_g^{(\text{HEF})}$ is governed by the right-most singularity of Eq. (15) in the N plane, namely at $N = \hat{\alpha}_s$. At $|\rho| \ll 1$, one thus has $\check{C}_g^{(\text{HEF})} \propto |\rho|^{-\hat{\alpha}_s-1}$. This type of *hard Pomeron* behaviour is absent in the case of the scale-fixing solution to the instability problem. In a complete LLA treatment [45–47], the value of the exponent would be $4\hat{\alpha}_s \ln 2$ instead $\hat{\alpha}_s$. Anticipating the comparison with the experimental data, we note that the larger LLA value of the Pomeron intercept would lead to an even more rapidly growing cross section, incompatible with the measurements.

3.2. Matching of the NLO and resummed CF results

So far, we have described two approximations for the CF coefficient function: the NLO CF of Sec. 2.2. and the DLA HEF of Sec. 3.1. Now we are in a position to combine them using a simple *subtractive-matching* prescription:

$$C_{g,q}^{(\text{match.})}(x, \xi) = C_{g,q}^{(0)}(x, \xi) + C_{g,q}^{(1)}(x, \xi) + [\check{C}_{g,q}^{(\text{HEF})}(\xi/|x|) - C_{g,q}^{(1, \text{asy.})}(x, \xi)]\theta(|x| - \xi). \quad (18)$$

For $\rho \rightarrow 0$ corresponding to $\xi \ll |x| < 1$, $C_{g,q}^{(1, \text{asy.})}(x, \xi) \simeq C_{g,q}^{(1)}(x, \xi)$ by definition. For $\rho \rightarrow 1$ corresponding to $\xi \lesssim x < 1$, $\check{C}_{g,q}^{(\text{HEF})}(\xi/|x|) \simeq C_{g,q}^{(1, \text{asy.})}(x, \xi)$ because all terms proportional to $\ln^n(1/|\rho|)$ in Eq. (16) tend to 0.

In both limits, the matched result is given by the approximation we trust the most: $C_{g,q}^{(\text{HEF})}$ from DLA HEF for $\rho \rightarrow 0$

and $C_{g,q}^{(0)} + C_{g,q}^{(1)}$ from NLO CF for $\rho \rightarrow 1$. The θ function in Eq. (18) indicates that the resummation is applicable only for $|x| > \xi$, namely the DGLAP region.

One of many other possible HEF-to-CF-matching prescriptions is the *inverse-error-weighting* (InEW) matching [12, 13, 53]. Since our calculations in the inclusive case indicated [12, 13] that the central values and scale variation bands of the cross sections obtained with the subtractive and InEW matchings were consistent within the InEW matching uncertainty, we chose to stick here to the simplest matching prescription, leaving the implementation of the InEW matching for a future work.

3.3. Resummed results

As we have done to illustrate the known problematic NLO CF behaviour [5], let us first examine the relative μ_F uncertainty of the NLO CF \oplus DLA HEF results for the t -differential cross section shown in Fig. 2a in red: its μ_F uncertainty remains roughly constant and below a factor of 3, unlike the LO (grey) and NLO (blue) ones. This illustrates the improvement through the matched HEF resummation.

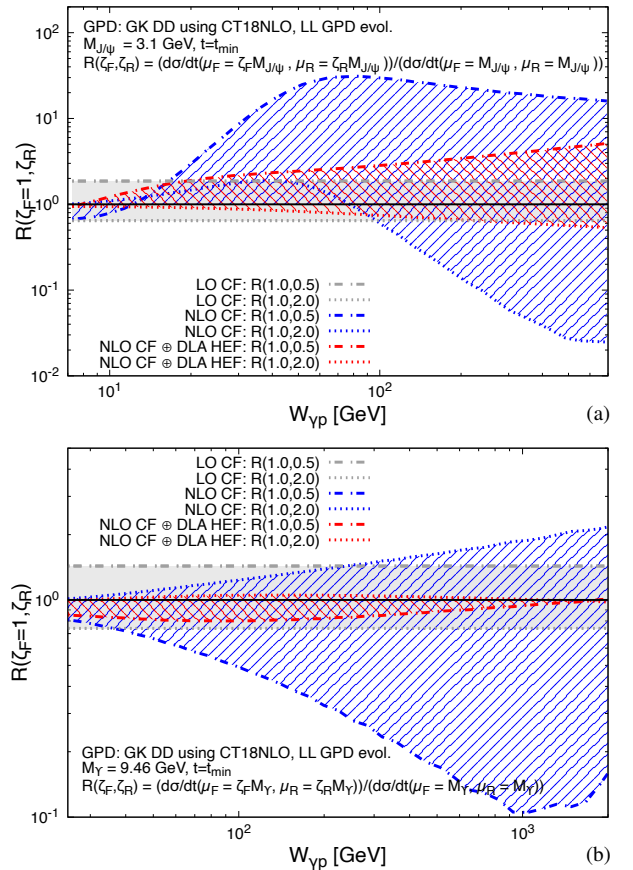


Figure 4: μ_R scale uncertainty of the LO CF, NLO CF and NLO CF \oplus DLA HEF (a) J/ψ and (b) Y t -differential cross sections.

Let us now turn to the μ_R variation/uncertainties of NLO CF \oplus DLA HEF compared to the expected energy-independent LO CF variation, and that of the NLO CF shown in Fig. 4.

⁷The subtraction is indicated by the \checkmark mark on C .

⁸ I_n (J_n) is the Bessel function of the second (first) kind and $\text{Li}_n(x)$ is the classic polylogarithm of order n .

For the J/ψ case (Fig. 4a), the NLO CF is again at odds with any expectations above $W_{\gamma p} \approx 20$ GeV. The NLO CF \oplus DLA HEF uncertainty is significantly smaller than the NLO CF one and slowly increases to become larger than the LO CF one above $W_{\gamma p} \approx 20$ GeV. This increase follows from the μ_R dependence of the hard-pomeron contribution, whose asymptotic behaviour in the DLA (Eq. (17)) directly depends on μ_R as $|\rho|^{-\hat{\alpha}_s(\mu_R)-1}$ without any compensation at this order. We expect a smaller sensitivity with a complete NLLA computation. For the Υ case (Fig. 4b), the NLO CF band is consistently broader than the LO CF one across the entire energy range shown and this broadening increases steadily with energy. Contrary to the J/ψ case, the NLO CF \oplus DLA HEF uncertainty does not increase and remains always (much) smaller than for the LO CF case. The aforementioned increase due to the hard-pomeron contribution is expected to set in at higher energies, even above what is accessible at a possible FCC-eh.

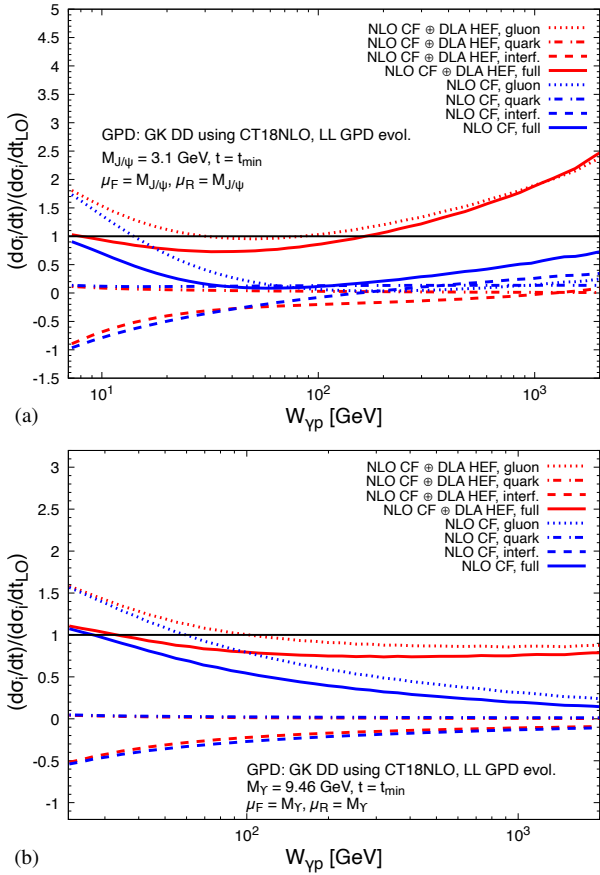


Figure 5: Decomposition of the NLO CF and NLO CF \oplus DLA HEF of the t -differential cross section (normalised to the LO one) into contributions coming from only quarks, only gluons and their interference for (a) J/ψ and (b) Υ .

In order to discuss the sensitivity of the cross section on the quark and gluon GPDs, one can decompose the cross section into the amplitude squared from quark-only (dash-dotted) and gluon-only (dotted) GPDs and their interference (dashed) as in Fig. 5. For the NLO CF (blue), one observes that the full contribution (solid) is suppressed by the negative interference and is such that the gluon-only con-

tribution becomes unnaturally small, even smaller than the quark-only contribution. This high-energy behaviour, noted in [54, 55] is due to the instability of the NLO CF contributions and should not be considered as physically sound. Therefore, in what follows, we will not show the NLO CF cross sections anymore. On the other hand, as also shown, the gluon-only contribution dominates the NLO CF \oplus DLA HEF cross section, restoring the LO picture of gluon dominance and thus exhibiting an improved stability.

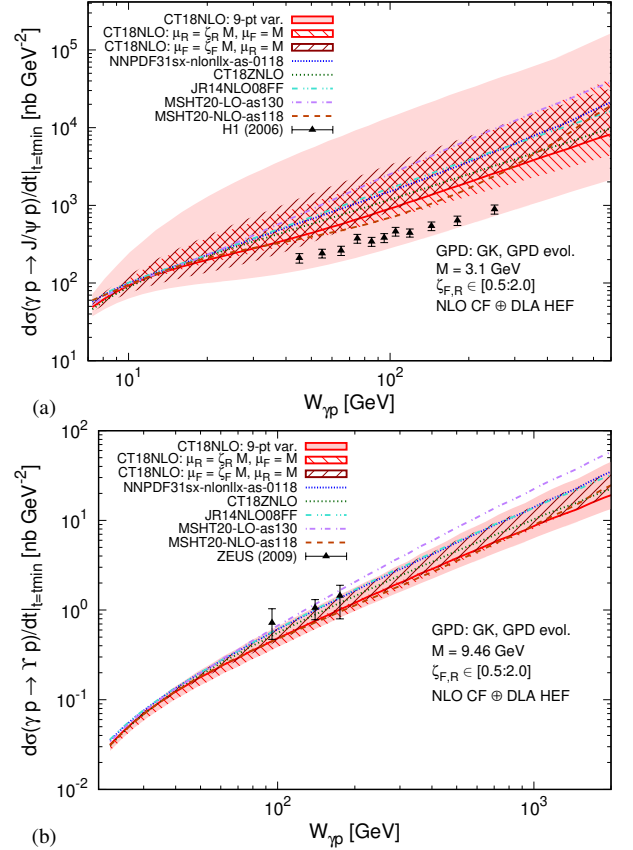


Figure 6: (a) NLO CF \oplus DLA HEF cross section as a function of $W_{\gamma p}$ using a variety of input GPDs. The 9-point variation band is shaded while the hatched bands correspond to the sole variations of either μ_F or μ_R with input CT18NLO GPDs. Also shown for comparison purposes is the most precise t -differential cross section data extrapolated down to $t = t_{\min}$ from the H1 collaboration [56]. (b) Same as (a) but for Υ production and t -differential cross section data extrapolated down to $t = t_{\min}$ from the ZEUS collaboration [57].

Having discussed the improvement brought about by the HEF resummation with regards to the stability of the cross section, we are now ready to compare our results to experimental data. As announced, we focus on the t -differential cross section at $t = t_{\min}$. To make our comparison even more accurate, instead of simply comparing our computation to the data in the smallest t bin, we have converted them to $t = t_{\min}$ extrapolating the measured t dependence at $\langle |t| \rangle = 0.03$ GeV 2 as follows $d\sigma/dt \propto \exp(-b(W_{\gamma p})t)$ with $b(W_{\gamma p})$ GeV $^2 = B_0 + 4\alpha'_{\mathbb{P}} \ln(W_{\gamma p}/90)$ and duly propagating the experimental uncertainties. We take $B_0 = 4.63$ and $\alpha'_{\mathbb{P}} = 0.164$ [56]. For the record, the obtained corrections is on the order of 15-20%. Our computed cross sections

are shown with an estimated uncertainty following from the 9-point scale variation⁹ about M_Q .

In addition, we have added to Fig. 6 results computed with the central eigenvector set of CT18ZNLO [23], an alternate CT18 fit with a different gluon PDF, as well as the LO set MSHT20-LO-as130 [58], another conventional NLO set MSHT20-NLO-as118 [58], as well as JR14NLO08FF [59] and NNPDF31sx-nlonllx-as-0118 [60], both known to be steeper at low x and low scales. It allows us to assess the uncertainty from the input PDF in our DD GPDs to be compared to the perturbative uncertainties evaluated from the scale variation.

For the J/ψ case, our (large) scale-uncertainty band shown in Fig. 6a is in agreement with the experimental data¹⁰ which tends to lie on the lower side. The coloured curves obtained for the central values of different PDF sets and with our central scale M_Q exhibit an uncertainty of $O(2 - 3)$ which is similar to the uncertainty from varying μ_F and μ_R separately. For Υ , shown in Fig. 6b, our band is again in agreement with the experimental data, with a similar spread in the central values at the largest energies shown. In this case, the PDF-input uncertainty is similar than the combined scale uncertainty from the 9-point scale variation.

4. Conclusions

In the present paper we have discussed exclusive vector-quarkonium production in the framework of CF at NLO supplemented by the resummation of a series of higher-order corrections in CF, which are crucial to resolve the perturbative instability of the NLO CF computation at $W_{\gamma p} \gg M_Q$. In our opinion, this approach is the most suitable in providing a uniformly accurate description of this observable over a wide energy range, in comparison to e.g. CGC [61], small- x [62] or k_T -factorisation [51] approaches, applicable only at high energies.

We have found that the resummation indeed cures the NLO CF perturbative instability with a smooth energy dependence in agreement with the experimental data. Our results also confirm that quarkonium photoproduction is predominantly gluon-induced with quark-induced contributions only arising from radiative corrections and at most at the level of 20% via interference with gluon-induced contributions for $W_{\gamma p} > 100$ GeV.

We think our study is an important milestone for future global fits of GPDs using quarkonium data. It also highlights that most of the observed features of the NLO CF and resummation results (e.g. scale and flavour dependencies) cannot be captured by reducing GPDs to a simple square of PDFs. Constraints on PDFs might however be obtained

⁹ μ_R and μ_F are independently set to $\mu_F = \mu_0 \times \zeta_F$ and $\mu_R = \mu_0 \times \zeta_R$, for $\zeta_{F,R} \in \{1/2, 1, 2\}$ and $\mu_0 = M_Q$. The filled band is the envelope of the corresponding cross sections. As a complement, we show the envelope corresponding to the sole variation of μ_F and μ_R with hatched bands.

¹⁰We however stress that the size of the uncertainty is a matter of convention as we could vary the scale by a different amount than 2.

from a global GPD fit with PDFs as forward inputs in a DD model for instance. Quantifying such sensitivity along with the expected experimental improvements at the LHC [63] or the EIC [64] is clearly beyond the scope of the present work.

Our results are limited by the large scale uncertainty in the J/ψ case (Fig. 6a), for which the dataset is the most extensive. The picture is more promising for Υ photoproduction (Fig. 6b), although the dataset is more restricted. We anticipate the scale uncertainty will be reduced once we develop this computation beyond the DLA (see e.g. [65]), which is the subject of a future work. Further improvement can be made by including relativistic- v^2 and/or higher-twist corrections in Λ_{QCD}/M_Q , which should be larger for J/ψ than for Υ production.

Acknowledgements.. We thank V. Bertone, D. Boer, V. Braun, J.R. Cudell, H. Dutrieux, K. Lynch, R. McNulty, H. Moutarde, M. Ozcelik, M. Ryskin, M. Strikman, L. Szymanowski, C. Van Hulse, S. Wallon, F. Yuan for useful discussions. This project has received funding from the European Union’s Horizon 2020 research and innovation programme under grant agreement No. 824093 in order to contribute to the EU Virtual Access NLOAccess and the JRA Fixed-Target Experiments at the LHC and a Marie Skłodowska-Curie action “RadCor4HEF” under grant agreement No. 101065263. This project has also received funding from the Agence Nationale de la Recherche (ANR) via the grant ANR-20-CE31-0015 (“PrecisOnium”) and via the IDEX Paris-Saclay “Investissements d’Avenir” (ANR-11-IDEX-0003-01) through the GLUODYNAMICS project funded by the “P2IO LabEx (ANR-10-LABX-0038)”. This work was also partly supported by the French CNRS via the IN2P3 projects “GLUE@NLO” and “QCD-Factorisation@NLO” as well as via the COPIN-IN2P3 project #12-147 “kT factorisation and quarkonium production in the LHC era”.

Appendix A. derivation of the HEF coefficient function

In this appendix we provide details of the derivation of the HEF coefficient function (13). Let us consider the one-loop amplitudes of the processes:

$$\gamma(q) + g(p_1) \rightarrow Q\bar{Q} \left[{}^3S_1^{[11]} \right] (p_Q) + g(p'_1), \quad (\text{A.1})$$

$$\gamma(q) + q(p_1) \rightarrow Q\bar{Q} \left[{}^3S_1^{[11]} \right] (p_Q) + q(p'_1), \quad (\text{A.2})$$

with typical diagrams shown in Fig. 7(a,b). One is interested in the imaginary part of these amplitudes in the Regge limit, when the partonic centre-of-mass energy $\hat{s} = (q + p_1)^2$ is much larger than $\hat{t} = (q - p_Q)^2 = t_{\text{min}}$ and M_Q^2 . The Regge asymptotics can be computed with the help of the following replacement for the Feynman-gauge t -channel gluon propagators highlighted in bold in Fig. 7:

$$\frac{-ig^{\mu\nu}}{k^2 + i\epsilon} \rightarrow \frac{i}{2\mathbf{k}_\perp^2} (n_-^\mu n_+^\nu + n_+^\mu n_-^\nu), \quad (\text{A.3})$$

where $n_+^\mu = 2q^\mu/\sqrt{\hat{s}}$ and $n_-^\mu = 2p_1^\mu/\sqrt{\hat{s}}$ are the Sudakov basis vectors¹¹ with $n^+ \cdot n^- = 2$. After this replacement, the one-loop gluon ($i = g$, Eq. (A.1)) or quark ($i = q$, Eq. (A.2)) amplitude can be factorised as:

$$i\mathcal{M}_{\gamma i} = -\frac{1}{2} \int \frac{d^{2-2\epsilon}\mathbf{l}_\perp}{(2\pi)^{4-2\epsilon}} \int \frac{dl_+ dl_-}{2} \frac{\mathcal{A}_{ab}(l_+, \mathbf{l}_\perp) \mathcal{B}_i^{ab}(l_-, \mathbf{l}_\perp)}{(2\mathbf{l}_\perp^2)^2}, \quad (\text{A.4})$$

with the the projectile (target) Impact Factors (IF) \mathcal{A}_{ab} (\mathcal{B}_i^{ab}) defined below. In the leading-power approximation w.r.t. $1/\hat{s}$, the l_+ integration gets routed through the projectile IF \mathcal{A}_{ab} , while the l_- integration goes through the target IF \mathcal{B}_i^{ab} . The result for the projectile IF before the l_+ integration is:

$$\mathcal{A}_{ab} = \frac{-32cq^2 \mathbf{l}_\perp^2 (\varepsilon^{*\mathcal{Q}} \cdot \varepsilon^\gamma)}{[2l_+ q_- - M_Q^2 - 4\mathbf{l}_\perp^2 + i\varepsilon][2l_+ q_- + M_Q^2 + 4\mathbf{l}_\perp^2 - i\varepsilon]}, \quad (\text{A.5})$$

where $\varepsilon^\gamma(q) \cdot p_1 = 0$, a, b are the colour indices of t -channel gluons and in the derivation we have used the following replacement for the spinors of outgoing heavy quark and antiquark with momenta $p_Q/2$:

$$u_\alpha^i \left(\frac{p_Q}{2} \right) \bar{v}_\beta^j \left(\frac{p_Q}{2} \right) \rightarrow \delta^{ij} \frac{[(\not{p}_Q - M_Q) \not{\varepsilon}^{*(\mathcal{Q})} (\not{p}_Q + M_Q)]_{\alpha\beta}}{4\sqrt{M_Q^2 N_c}}, \quad (\text{A.6})$$

to project their colour (i, j) and Dirac (α, β) indices on the colour-singlet state with the total spin equal to one. Integrating out the l_+ momentum in the projectile IF gives us the HEF coefficient function (13) as expected:

$$\int_{-\infty}^{+\infty} dl_+ \mathcal{A}_{ab}(l_+, \mathbf{l}_\perp) = 8i\delta_{ab} (\varepsilon^{*\mathcal{Q}} \cdot \varepsilon^\gamma) \frac{q_- \mathbf{l}_\perp^2}{m_Q^2} h(\mathbf{l}_\perp^2). \quad (\text{A.7})$$

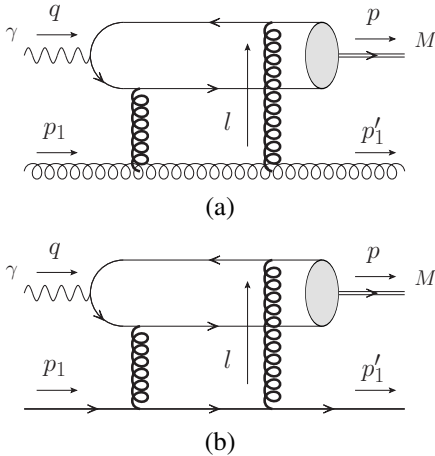


Figure 7: Typical Feynman diagrams contributing to the imaginary part of the amplitude in the gluon-target (a) and quark-target (b) case. All 6 possible diagrams should be included.

To project the gluon-target IF on the CF coefficient function in Eq. (8), we replace the polarisation vectors of the

¹¹We define the Sudakov decomposition for any vector $k^\mu = (k^+ n_+^\mu + k^- n_-^\mu)/2 + k_\perp^\mu$ with $n_\pm \cdot k_\perp = 0$, $k^\pm = n_\pm \cdot k$ such that $k^2 = k_+ k_- - \mathbf{k}_\perp^2$.

target gluons as follows:

$$\varepsilon_\mu(p_1) \varepsilon_\nu^*(p_1') \rightarrow \frac{\delta_{ab}}{(N_c^2 - 1)} \frac{-g_{\mu\nu} + (n_+^\mu n_-^\nu + n_-^\mu n_+^\nu)/2}{2(D - 2)}, \quad (\text{A.8})$$

with $D = 4 - 2\epsilon$ being the spacetime dimension, while for target quarks the corresponding replacement for spinors is:

$$u_\alpha^i(p_1') \bar{u}_\beta^j(p_1) \rightarrow \frac{\delta_{ij}}{N_c} \frac{(\not{p}_1)_{\alpha\beta}}{2x}. \quad (\text{A.9})$$

In the CF kinematics, $p_1^\mu = xP^\mu$ with P being the proton momentum and $\xi \ll |x| \lesssim 1$ in the $|\rho| \ll 1$ region we are interested in. With these substitutions, the result for the target IFs before the l_- integration are:

$$\mathcal{B}_g^{ab} = -\frac{4N_c \delta^{ab} g_s^2}{N_c^2 - 1} \frac{(p_1^+)^2 \mathbf{l}_\perp^2}{(l_- p_1^+ + \mathbf{l}_\perp^2 - i\varepsilon)(l_- p_1^+ - \mathbf{l}_\perp^2 + i\varepsilon)}, \quad (\text{A.10})$$

$$\mathcal{B}_q^{ab}(l_-, \mathbf{l}_\perp) = \frac{2C_F}{xC_A} \mathcal{B}_g^{ab}(l_-, \mathbf{l}_\perp), \quad (\text{A.11})$$

while the gluon IF after integrating-out l_- gives:

$$\int_{-\infty}^{\infty} dl_- \mathcal{B}_g^{ab}(l_-, \mathbf{l}_\perp) = 4\pi i g_s^2 \frac{N_c \delta^{ab}}{N_c^2 - 1} |p_1^+|. \quad (\text{A.12})$$

Substituting these results into Eq. (A.4), one obtains the imaginary part of the NLO CF gluon coefficient function in the Regge limit $|\rho| \ll 1$ in the following form:

$$\text{Im } C_g^{(\text{NLO})}(\rho \ll 1) = -\frac{r_\Gamma}{|\rho|} \int_0^{\infty} d\mathbf{l}_\perp^2 \left(\frac{\mu^2}{\mathbf{l}_\perp^2} \right)^\epsilon \left\{ \hat{\alpha}_s \right\} h(\mathbf{l}_\perp^2), \quad (\text{A.13})$$

where $r_\Gamma = (4\pi)^\epsilon/\Gamma(1 - \epsilon)$. On the one hand, integrating out the \mathbf{l}_\perp^2 in the last equation and subtracting the collinear pole according to the $\overline{\text{MS}}$ scheme, one recovers the asymptotic result (10). On the other hand, Eq. (A.13) at $\epsilon = 0$ has the form of Eq. (12) with the factor in the curly brackets in Eq. (A.13) being nothing but the $O(\alpha_s)$ term in the expansion of the resummation factor (14). The last observation fixes the overall factor in Eq. (12) for both the quark and gluon cases.

Finally, we give a hint for the derivation of Eq. (17). The Mellin transform of Eq. (15) can be rewritten as an integral over $\gamma = \hat{\alpha}_s/N$:

$$C_g^{(\text{HEF})}(\rho) = \frac{-i\pi c}{2} \frac{\hat{\alpha}_s}{|\rho|} \sum_{n=0}^{\infty} \frac{L_\rho^n}{n!} \oint \frac{d\gamma}{2\pi i} \gamma^{-n-2} e^{\gamma L_\rho} \frac{\pi\gamma}{\sin(\pi\gamma)},$$

where we have used the series expansion of $e^{L_\rho/\gamma}$. The contour in the γ plane encircles the singularity at $\gamma = 0$ but can be blown-up to encircle poles at positive and negative integer points instead which, after summing all the residues, gives $(-1)^{n+1} [\text{Li}_{n+1}(-e^{-L_\rho}) + (-1)^{n+1} \text{Li}_{n+1}(-e^{L_\rho})]$ for the γ integral. This combination of polylogarithms can be rewritten in terms of logarithms using the identity [66]:

$$\text{Li}_n(z) + (-1)^n \text{Li}_n\left(\frac{1}{z}\right) = -\frac{\ln^n(-z)}{n!} + 2 \sum_{k=1}^{\lfloor \frac{n}{2} \rfloor} \frac{\text{Li}_{2k}(-1)}{(n-2k)!} \ln^{n-2k}(-z),$$

which after swapping the order of summations over n and k and summing the infinite series in n into Bessel functions, gives Eq. (17).

References

- [1] A. V. Radyushkin, “Nonforward parton distributions,” *Phys. Rev. D* **56** (1997) 5524–5557, [arXiv:hep-ph/9704207](#).
- [2] M. Burkardt, “Impact parameter dependent parton distributions and off forward parton distributions for $zeta \rightarrow 0$,” *Phys. Rev. D* **62** (2000) 071503, [arXiv:hep-ph/0005108](#). [Erratum: *Phys.Rev.D* **66**, 119903 (2002)].
- [3] M. Burkardt, “Impact parameter space interpretation for generalized parton distributions,” *Int. J. Mod. Phys. A* **18** (2003) 173–208, [arXiv:hep-ph/0207047](#).
- [4] J. C. Collins, L. Frankfurt, and M. Strikman, “Factorization for hard exclusive electroproduction of mesons in QCD,” *Phys. Rev. D* **56** (1997) 2982–3006, [arXiv:hep-ph/9611433](#).
- [5] D. Y. Ivanov, A. Schafer, L. Szymanowski, and G. Krasnikov, “Exclusive photoproduction of a heavy vector meson in QCD,” *Eur. Phys. J. C* **34** no. 3, (2004) 297–316, [arXiv:hep-ph/0401131](#). [Erratum: *Eur.Phys.J.C* **75**, 75 (2015)].
- [6] C. A. Flett, J. A. Gracey, S. P. Jones, and T. Teubner, “Exclusive heavy vector meson electroproduction to NLO in collinear factorisation,” *JHEP* **08** (2021) 150, [arXiv:2105.07657 \[hep-ph\]](#).
- [7] G. A. Schuler, “Quarkonium production and decays,” 1994.
- [8] M. L. Mangano and A. Petrelli, “NLO quarkonium production in hadronic collisions,” *Int. J. Mod. Phys. A* **12** (1997) 3887–3897, [arXiv:hep-ph/9610364](#).
- [9] Y. Feng, J.-P. Lansberg, and J.-X. Wang, “Energy dependence of direct-quarkonium production in pp collisions from fixed-target to LHC energies: complete one-loop analysis,” *Eur. Phys. J. C* **75** no. 7, (2015) 313, [arXiv:1504.00317 \[hep-ph\]](#).
- [10] J.-P. Lansberg and M. A. Ozelik, “Curing the unphysical behaviour of NLO quarkonium production at the LHC and its relevance to constrain the gluon PDF at low scales,” *Eur. Phys. J. C* **81** no. 6, (2021) 497, [arXiv:2012.00702 \[hep-ph\]](#).
- [11] A. C. Serri, Y. Feng, C. Flore, J.-P. Lansberg, M. A. Ozelik, H.-S. Shao, and Y. Yedelkina, “Revisiting NLO QCD corrections to total inclusive J/ψ and Upsilon photoproduction cross sections in lepton-proton collisions,” [arXiv:2112.05060 \[hep-ph\]](#).
- [12] J.-P. Lansberg, M. Nefedov, and M. A. Ozelik, “Matching next-to-leading-order and high-energy-resummed calculations of heavy-quarkonium-hadroproduction cross sections,” *JHEP* **05** (2022) 083, [arXiv:2112.06789 \[hep-ph\]](#).
- [13] J.-P. Lansberg, M. Nefedov, and M. A. Ozelik, “Curing the high-energy perturbative instability of vector-quarkonium-photoproduction cross sections at order α_s^3 with high-energy factorisation,” *Eur. Phys. J. C* **84** no. 4, (2024) 351, [arXiv:2306.02425 \[hep-ph\]](#).
- [14] S. P. Jones, A. D. Martin, M. G. Ryskin, and T. Teubner, “Exclusive J/ψ and Υ photoproduction and the low x gluon,” *J. Phys. G* **43** no. 3, (2016) 035002, [arXiv:1507.06942 \[hep-ph\]](#).
- [15] X.-D. Ji, “Off forward parton distributions,” *J. Phys. G* **24** (1998) 1181–1205, [arXiv:hep-ph/9807358](#).
- [16] K. Goeke, M. V. Polyakov, and M. Vanderhaeghen, “Hard exclusive reactions and the structure of hadrons,” *Prog. Part. Nucl. Phys.* **47** (2001) 401–515, [arXiv:hep-ph/0106012](#).
- [17] A. V. Belitsky, D. Mueller, and A. Kirchner, “Theory of deeply virtual Compton scattering on the nucleon,” *Nucl. Phys. B* **629** (2002) 323–392, [arXiv:hep-ph/0112108](#).
- [18] A. V. Radyushkin, “Double distributions and evolution equations,” *Phys. Rev. D* **59** (1999) 014030, [arXiv:hep-ph/9805342](#).
- [19] A. V. Radyushkin, “Symmetries and structure of skewed and double distributions,” *Phys. Lett. B* **449** (1999) 81–88, [arXiv:hep-ph/9810466](#).
- [20] I. V. Musatov and A. V. Radyushkin, “Evolution and models for skewed parton distributions,” *Phys. Rev. D* **61** (2000) 074027, [arXiv:hep-ph/9905376](#).
- [21] S. V. Goloskokov and P. Kroll, “The Longitudinal cross-section of vector meson electroproduction,” *Eur. Phys. J. C* **50** (2007) 829–842, [arXiv:hep-ph/0611290](#).
- [22] J. Pumplin, D. R. Stump, J. Huston, H. L. Lai, P. M. Nadolsky, and W. K. Tung, “New generation of parton distributions with uncertainties from global QCD analysis,” *JHEP* **07** (2002) 012, [arXiv:hep-ph/0201195](#).
- [23] T.-J. Hou *et al.*, “New CTEQ global analysis of quantum chromodynamics with high-precision data from the LHC,” *Phys. Rev. D* **103** no. 1, (2021) 014013, [arXiv:1912.10053 \[hep-ph\]](#).
- [24] B. Berthou *et al.*, “PARTONS: PARTonic Tomography Of Nucleon Software: A computing framework for the phenomenology of Generalized Parton Distributions,” *Eur. Phys. J. C* **78** no. 6, (2018) 478, [arXiv:1512.06174 \[hep-ph\]](#).
- [25] V. Bertone, “APFEL++: A new PDF evolution library in C++,” *PoS DIS2017* (2018) 201, [arXiv:1708.00911 \[hep-ph\]](#).
- [26] V. Bertone, H. Dutrieux, C. Mezrag, J. M. Morgado, and H. Moutarde, “Revisiting evolution equations for generalised parton distributions,” *Eur. Phys. J. C* **82** no. 10, (2022) 888, [arXiv:2206.01412 \[hep-ph\]](#).
- [27] M. V. Polyakov and C. Weiss, “Skewed and double distributions in pion and nucleon,” *Phys. Rev. D* **60** (1999) 114017, [arXiv:hep-ph/9902451](#).
- [28] H1 Collaboration, C. Alexa *et al.*, “Elastic and Proton-Dissociative Photoproduction of J/ψ Mesons at HERA,” *Eur. Phys. J. C* **73** no. 6, (2013) 2466, [arXiv:1304.5162 \[hep-ex\]](#).
- [29] E. J. Eichten and C. Quigg, “Quarkonium wave functions at the origin,” *Phys. Rev. D* **52** (1995) 1726–1728, [arXiv:hep-ph/9503356](#).
- [30] E. J. Eichten and C. Quigg, “Quarkonium wave functions at the origin: an update,” [arXiv:1904.11542 \[hep-ph\]](#).
- [31] B. Schmidt and M. Steinhauser, “CRUNDEC: a C++ package for running and decoupling of the strong coupling and quark masses,” *Comput. Phys. Commun.* **183** (2012) 1845–1848, [arXiv:1201.6149 \[hep-ph\]](#).
- [32] C. A. Flett, S. P. Jones, A. D. Martin, M. G. Ryskin, and T. Teubner, “How to include exclusive J/ψ production data in global PDF analyses,” *Phys. Rev. D* **101** no. 9, (2020) 094011, [arXiv:1908.08398 \[hep-ph\]](#).
- [33] C. A. Flett, A. D. Martin, M. G. Ryskin, and T. Teubner, “Very low x gluon density determined by LHCb exclusive J/ψ data,” *Phys. Rev. D* **102** (2020) 114021, [arXiv:2006.13857 \[hep-ph\]](#).
- [34] C. A. Flett, S. P. Jones, A. D. Martin, M. G. Ryskin, and T. Teubner, “Exclusive J/ψ and Υ production in high energy pp and pPb collisions,” *Phys. Rev. D* **106** no. 7, (2022) 074021, [arXiv:2206.10161 \[hep-ph\]](#).
- [35] A. G. Shuvaev, K. J. Golec-Biernat, A. D. Martin, and M. G. Ryskin, “Off diagonal distributions fixed by diagonal partons at small x and x_i ,” *Phys. Rev. D* **60** (1999) 014015, [arXiv:hep-ph/9902410](#).
- [36] A. Shuvaev, “Solution of the off forward leading logarithmic evolution equation based on the Gegenbauer moments inversion,” *Phys. Rev. D* **60** (1999) 116005, [arXiv:hep-ph/9902318](#).
- [37] H. Dutrieux, M. Winn, and V. Bertone, “Exclusive meets inclusive particle production at small Bjorken x_B : How to relate exclusive measurements to PDFs based on evolution equations,” *Phys. Rev. D* **107** no. 11, (2023) 114019, [arXiv:2302.07861 \[hep-ph\]](#).
- [38] D. Y. Ivanov, “Exclusive vector meson electroproduction,” in *12th International Conference on Elastic and Diffractive Scattering: Forward Physics and QCD*, pp. 26–32. 12, 2007. [arXiv:0712.3193 \[hep-ph\]](#).
- [39] S. Catani, M. Ciafaloni, and F. Hautmann, “GLUON CONTRIBUTIONS TO SMALL x HEAVY FLAVOR PRODUCTION,” *Phys. Lett. B* **242** (1990) 97–102.
- [40] S. Catani, M. Ciafaloni, and F. Hautmann, “High-energy factorization and small x heavy flavor production,” *Nucl. Phys. B* **366** (1991) 135–188.
- [41] J. C. Collins and R. K. Ellis, “Heavy quark production in very high-energy hadron collisions,” *Nucl. Phys.* **B360** (1991) 3–30.
- [42] S. Catani and F. Hautmann, “High-energy factorization and small x deep inelastic scattering beyond leading order,” *Nucl. Phys.* **B427** (1994) 475–524, [arXiv:hep-ph/9405388 \[hep-ph\]](#).
- [43] L. N. Lipatov, “Gauge invariant effective action for high-energy processes in QCD,” *Nucl. Phys.* **B452** (1995) 369–400.
- [44] S. Caron-Huot, “When does the gluon reggeize?,” *JHEP* **05** (2015) 093, [arXiv:1309.6521 \[hep-th\]](#).
- [45] E. A. Kuraev, L. N. Lipatov, and V. S. Fadin, “Multi - Reggeon processes in the Yang-Mills theory,” *Sov. Phys. JETP* **44** (1976) 443.
- [46] E. A. Kuraev, L. N. Lipatov, and V. S. Fadin, “The Pomeron singularity in non-Abelian gauge theories,” *Sov. Phys. JETP* **45**

- (1977) 199.
- [47] Y. Y. Balitsky and L. N. Lipatov, “The Pomernanchuk singularity in Quantum Chromodynamics,” *Sov. J. Nucl. Phys.* **28** (1978) 822.
 - [48] V. S. Fadin, R. Fiore, M. I. Kotsky, and A. Papa, “Strong bootstrap conditions,” *Phys. Lett.* **B495** (2000) 329–337.
 - [49] V. S. Fadin, M. G. Kozlov, and A. V. Reznichenko, “Gluon Reggeization in Yang-Mills Theories,” *Phys. Rev.* **D92** no. 8, (2015) 085044, [arXiv:1507.00823 \[hep-th\]](#).
 - [50] D. Y. Ivanov, B. Pire, L. Szymanowski, and J. Wagner, “Probing GPDs in photoproduction processes at hadron colliders,” in *International Conference on the Structure and Interactions of the Photon and 21st International Workshop on Photon-Photon Collisions and International Workshop on High Energy Photon Linear Colliders*. 10, 2015. [arXiv:1510.06710 \[hep-ph\]](#).
 - [51] S. P. Jones, A. D. Martin, M. G. Ryskin, and T. Teubner, “Probes of the small x gluon via exclusive J/ψ and Υ production at HERA and the LHC,” *JHEP* **11** (2013) 085, [arXiv:1307.7099 \[hep-ph\]](#).
 - [52] J. Blumlein, “On the $k(T)$ dependent gluon density of the proton,” in *Deep inelastic scattering and QCD. Proceedings, Workshop, Paris, France, April 24-28, 1995*, pp. 265–268. 1995. [arXiv:hep-ph/9506403 \[hep-ph\]](#). <http://www-library.desy.de/cgi-bin/showprep.pl?desy95-121>.
 - [53] M. G. Echevarria, T. Kasemets, J.-P. Lansberg, C. Pisano, and A. Signori, “Matching factorization theorems with an inverse-error weighting,” *Phys. Lett. B* **781** (2018) 161–168, [arXiv:1801.01480 \[hep-ph\]](#).
 - [54] K. J. Eskola, C. A. Flett, V. Guzey, T. Löytäinen, and H. Paukkunen, “Exclusive J/ψ photoproduction in ultraperipheral Pb+Pb collisions at the CERN Large Hadron Collider calculated at next-to-leading order perturbative QCD,” *Phys. Rev. C* **106** no. 3, (2022) 035202, [arXiv:2203.11613 \[hep-ph\]](#).
 - [55] K. J. Eskola, C. A. Flett, V. Guzey, T. Löytäinen, and H. Paukkunen, “Next-to-leading order perturbative QCD predictions for exclusive J/ψ photoproduction in oxygen-oxygen and lead-lead collisions at energies available at the CERN Large Hadron Collider,” *Phys. Rev. C* **107** no. 4, (2023) 044912, [arXiv:2210.16048 \[hep-ph\]](#).
 - [56] H1 Collaboration, A. Aktas *et al.*, “Elastic J/ψ production at HERA,” *Eur. Phys. J. C* **46** (2006) 585–603, [arXiv:hep-ex/0510016](#).
 - [57] ZEUS Collaboration, S. Chekanov *et al.*, “Exclusive photoproduction of ϵ mesons at HERA,” *Phys. Lett. B* **680** (2009) 4–12, [arXiv:0903.4205 \[hep-ex\]](#).
 - [58] S. Bailey, T. Cridge, L. A. Harland-Lang, A. D. Martin, and R. S. Thorne, “Parton distributions from LHC, HERA, Tevatron and fixed target data: MSHT20 PDFs,” *Eur. Phys. J. C* **81** no. 4, (2021) 341, [arXiv:2012.04684 \[hep-ph\]](#).
 - [59] P. Jimenez-Delgado and E. Reya, “Delineating parton distributions and the strong coupling,” *Phys. Rev. D* **89** no. 7, (2014) 074049, [arXiv:1403.1852 \[hep-ph\]](#).
 - [60] R. D. Ball, V. Bertone, M. Bonvini, S. Marzani, J. Rojo, and L. Rottoli, “Parton distributions with small- x resummation: evidence for BFKL dynamics in HERA data,” *Eur. Phys. J. C* **78** no. 4, (2018) 321, [arXiv:1710.05935 \[hep-ph\]](#).
 - [61] H. Mäntysaari and J. Penttala, “Complete calculation of exclusive heavy vector meson production at next-to-leading order in the dipole picture,” *JHEP* **08** (2022) 247, [arXiv:2204.14031 \[hep-ph\]](#).
 - [62] D. Boer and C. Setyadi, “Probing gluon GTMDs through exclusive coherent diffractive processes,” *Eur. Phys. J. C* **83** no. 10, (2023) 890, [arXiv:2301.07980 \[hep-ph\]](#).
 - [63] E. Chapon *et al.*, “Perspectives for quarkonium studies at the high-luminosity LHC,” [arXiv:2012.14161 \[hep-ph\]](#).
 - [64] D. Boer *et al.*, “Physics case for quarkonium studies at the Electron Ion Collider,” [arXiv:2409.03691 \[hep-ph\]](#).
 - [65] M. Nefedov, “One-loop impact factors for heavy quarkonium production: S -wave case,” [arXiv:2408.06234 \[hep-ph\]](#).
 - [66] <http://functions.wolfram.com/10.08.17.0010.01>.